

Removal of organic contaminants by RO and NF membranes

Yeomin Yoon, Richard M. Lueptow*

Department of Mechanical Engineering, Northwestern University, 2145 Sheridan Road, Evanston, IL 60208-3111, USA

Received 11 January 2005; received in revised form 17 March 2005; accepted 21 March 2005

Available online 29 April 2005

Abstract

Rejection characteristics of organic and inorganic compounds were examined for six reverse osmosis (RO) membranes and two nanofiltration (NF) membranes that are commercially available. A batch stirred-cell was employed to determine the membrane flux and the solute rejection for solutions at various concentrations and different pH conditions. The results show that for ionic solutes the degree of separation is influenced mainly by electrostatic exclusion, while for organic solutes the removal depends mainly upon the solute radius and molecular structure. In order to provide a better understanding of rejection mechanisms for the RO and NF membranes, the ratio of solute radius ($r_{i,s}$) to effective membrane pore radius (r_p) was employed to compare rejections. An empirical relation for the dependence of the rejection of organic compounds on the ratio $r_{i,s}/r_p$ is presented. The rejection for organic compounds is over 75% when $r_{i,s}/r_p$ is greater than 0.8. In addition, the rejection of organic compounds is examined using the extended Nernst–Planck equation coupled with a steric hindrance model. The transport of organic solutes is controlled mainly by diffusion for the compounds that have a high $r_{i,s}/r_p$ ratio, while convection is dominant for compounds that have a small $r_{i,s}/r_p$ ratio.

© 2005 Elsevier B.V. All rights reserved.

Keywords: Organic compounds; Reverse osmosis; Nanofiltration; Membrane pore radius; Water treatment

1. Introduction

The effective removal of organic compounds has always been a major challenge for the production of potable water, since the United States Environmental Protection Agency assessed the hazard of over 85,000 chemicals [1]. Although there are currently no federal regulations for most of these chemicals in drinking water, drinking water must be essentially free from organics in order to be fit for human consumption. However, there are few studies of how to remove the many unregulated chemicals based upon conventional and advanced drinking water treatment technologies including coagulation, softening, activated carbon, ion exchange, oxidation (e.g., chlorination and ozonation), and membrane filtration. For the last few decades, the use of membrane technology has grown significantly in the water industry compared to other water treatment technologies, since membrane filtration requires minimal addition of aggressive chemicals

and produces no problematic by-products. In particular, reverse osmosis (RO) including low pressure RO (LPRO) and nanofiltration (NF) are broadly used membrane processes for both potable water treatment and wastewater reuse [2–4].

Previous studies have shown that RO and NF are effective technologies to remove organic compounds when the solute sizes are larger than the membrane pore sizes or organic compounds have ionizable functional groups causing electrostatic repulsion [5–10]. However, these previous studies have typically considered relatively large compounds (e.g., molecular weight (MW) > 150 g/mol) and/or relatively hydrophobic compounds (e.g., logarithm of octanol–water partition coefficient > 2.0). Only a few studies have investigated the rejection of small uncharged organic compounds by RO and NF membranes [11–13]. These studies have shown that the rejections for uncharged small molecules such as urea are quite low. Like urea, other small, hydrophilic, uncharged molecules such as methanol and formaldehyde may also be quite difficult to remove using RO or NF membranes. However, few systematic measurements of the interaction of small organic molecules with RO and NF membranes are available.

* Corresponding author. Tel.: +1 847 491 4265; fax: +1 847 491 3915.
E-mail address: r-lueptow@northwestern.edu (R.M. Lueptow).

A complete understanding of the transport of small organic compounds through RO and NF membranes is a challenging issue, since solute transport depends on physico-chemical properties of the solvent, solute, and membrane. Factors include the solution pH and ionic strength, the solute size or shape and polarity or hydrophobicity, and the membrane pore size and charge.

Although our study focuses mainly on the rejection of organic compounds by RO and NF membranes, it is still necessary to evaluate the rejection of ionic compounds, since various ionic compounds always coexist in drinking source water. For inorganic compounds the solution pH and the membrane charge are major factors that influence the solute rejection due to electrostatic repulsion between ionic compounds and a charged membrane. Previous studies have shown that the rejection of sodium, calcium, chloride, and sulfate ions increases with increasing solution pH for the RO and NF membranes [14,15]. In these studies, solute concentration also influences the solute transport through the RO and NF membranes, since the membrane charge becomes more negative with increasing solution pH and with decreasing solute concentration. In addition, separate studies have shown that the rejection of both inorganic and organic compounds and the flux for the RO and NF membranes are significantly influenced by hydrodynamic operating parameters such as the water recovery (the ratio of total permeate volume to initial feed volume) and the volumetric concentration factor (the ratio of feed volumetric to concentrate volume) [11,12,16].

Several recent studies have investigated the transport mechanisms of ionic and organic solutes through RO or NF membranes [3,5,6,12,13,15]. These studies have shown that for organic compounds the removal depends upon the solute size/shape and polarity/hydrophobicity, while for ionic compounds the degree of separation is governed by both size exclusion and electrostatic exclusion. However, these studies are still limited to a few membranes and cover only a few inorganic or organic solutes. Therefore, a systematic rejection assessment both for organic and inorganic compounds is useful in order to investigate the rejection and transport mechanisms (i.e., diffusion, electromigration, and convection) for RO and NF membranes.

The objective of this study is to understand the physico-chemical processes related to the rejection of small uncharged organic compounds by RO and NF membranes. To accomplish this, the rejections of both organic and inorganic species were measured at various pH and recovery conditions. The experimental rejection data were analyzed using the extended Nernst–Planck equation to determine the dominant transport mechanisms as a function of ratio of solute radius to effective membrane pore radius and the diffusion in the membrane.

2. Materials and methods

Six RO membranes and two NF membranes that are commercially available were tested to measure the organic and inorganic rejections. The flat sheet, thin film composite membranes were obtained from different manufacturers, listed in Table 1. The typical operating pH recommended for the membranes ranges from 2 to 11. The normal/maximum operating pressures are 1035–1550/4140 kPa for the RO membranes and 518–690/4140 kPa for the NF membranes. The pure water permeabilities measured at 800 kPa using a stirred cell range from 0.51 to 2.36 L/d m² kPa.

Although the methods used in this paper and the results that have been obtained are generally applicable to removal of organic contaminants from water, we focus here on contaminants that typically are present in the cabin humidity condensate of a spacecraft [17]. This condensate water is often thought to be an ideal candidate for reuse as potable water for long-term space missions. However, it is often contaminated by organic chemicals, primarily due to off-gassing of polymer compounds in the spacecraft [18].

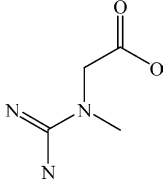
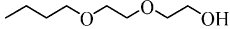
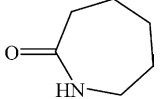
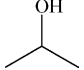
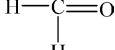
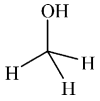
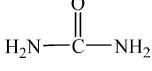
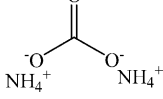
Initial screening tests were performed with solutions at concentrations of 1000 mg/L for sodium chloride (NaCl), 2000 mg/L for urea, and 3429 mg/L for ammonium carbonate ((NH₄)₂CO₃). The chemical composition of these solutions is based upon analysis of wastewater streams expected on board a spacecraft. They represent a mixed wastewater stream before and after ammonification of urea. For these screening tests, the criteria include high membrane flux and high rejection. For the three best membranes based upon the screening tests in each category considered (RO, LPRO,

Table 1
RO and NF membranes and their characteristics obtained from manufacturers

Membrane type/use	Membrane		pH range	Normal/maximum operating pressure (kPa)	Pure water permeability (L/d m ² kPa) ^a
	Product name	Manufacturer			
RO/surface water	AK	Desal-Osmonics	4–11	1550/NA	2.07
RO/low pressure	ESPA	Hydranautics	4–11	1035/4140	1.69
RO/brackish water	AG	Desal-Osmonics	4–11	1550/NA	0.96
RO/brackish water	70LW	Toray	3–9	1550/4140	0.71
RO/surface water	CAP	Hydranautics	4–11	1550/4140	0.58
RO/wastewater	LFC	Hydranautics	3–10	1550/4140	0.51
NF/water softening	HL	Desal-Osmonics	3–9	690/NA	2.36
NF/surface water	ESNA	Hydranautics	2–10	518/4140	1.38

^a Data obtained from dead-end stirred-cell experiments; NA: not available.

Table 2
List of target compounds used in this study [25,26]

Compound	MW (g/mol)	D_i (10^{-10} m ² /s)	Radius (nm)	Structure/formula
Creatine	131.2	6.6	0.37	
2-(2-Butoxyethoxy) ethanol	162.2	7.7	0.32	
Caprolactam	113.2	8.7	0.28	
2-Propanol	60.1	9.3	0.26	
Formaldehyde	30.0	11.1	0.22	
Methanol	32.0	12.8	0.19	
Urea	60.1	13.8	0.18	
Ammonium carbonate	96.1	Cation: 19.6; anion: 18.5; 19.2 ^a	Cation: 0.125; anion: 0.133	
Sodium chloride	58.5	Cation: 13.3; anion: 20.3; 16.1 ^a	Cation: 0.184; anion: 0.121	NaCl

^a Effective diffusion coefficient (D_{eff}).

and NF), the rejection was measured for the seven organic compounds and two inorganic compounds listed in Table 2. These organic and inorganic compounds are typically found in spacecraft wastewater [19] as well as in many other situations [20–22]. The organic compounds that are included in this study are creatine, 2-(2-butoxyethoxy)ethanol, caprolactam, 2-propanol, formaldehyde, methanol, and urea. The inorganic compounds include NaCl and $(\text{NH}_4)_2\text{CO}_3$. The test solutions were prepared by adding a single organic or inorganic species to distilled water at a concentration of 1 mM.

The experiments were performed in batch mode using a dead-end stirred cell that has been widely used for the various membrane filtration studies [5,7,12,13]. The stirred cell was made of aluminum and coated with Teflon to improve chemical stability by minimizing unnecessary interactions (e.g., adsorption) between solute and stirred cell. The cell had an active filtration area of 22.9 cm² and a working volume of 50 mL [13]. All the experiments were conducted at a stirring speed of 400 rpm, controlled by a magnetic stirrer (Stirrer assembly 8200, Millipore, USA), and a constant working pressure of 800 kPa, controlled by a high-pressure nitrogen cylinder and a gas pressure regulator.

A fresh membrane was used for each experiment. The membrane was soaked in ultra-pure deionized water at least

for 24 h to clean any chemicals on the membrane. During this period the pure water was replaced several times with a new volume of pure water. The dissolved organic carbon (DOC) of the final rinse water was checked to assure that it was at a negligible level. Additionally, the membrane was prefiltered with pure water at a pressure of 1380 kPa (200 psi) for further stabilization prior to use. The pure water flux was then measured at a pressure of 800 kPa (116 psi) until a constant flux was obtained. Only then was water in the stirred cell replaced by the test solution. The stability of the membrane permeability during the experiment was checked by comparing the pure water flux before and after each experiment. Only those membranes for which permeability changes were less than 5% were included in the data presented here.

The weight of the permeate was measured using a balance. The permeate flux is expressed in terms of volumetric concentration factor (f_c),

$$f_c = \frac{V_f}{V_c} = 1 + \frac{V_p}{V_c} \quad (1)$$

where V_f , V_c and V_p are defined as the volume of feed, concentrate, and permeate, respectively. The volumetric concentration factor has been widely used as a comparable hydrodynamic operating parameter for the membrane filtration

studies [12,16]. The solute concentrations of the permeate were measured at different volumetric concentration factors.

The rejection for species i , R_i , was calculated as:

$$R_i (\%) = \left(1 - \frac{C_p}{C_f}\right) \times 100 \quad (2)$$

where C_p is the permeate concentration and C_f the concentration in the feed (bulk) solution. The concentration in the permeate was measured several times until $f_c = 1.0$ – 2.5 corresponding to a recovery of 0–60%. After filtration tests, samples were acidified below a pH of 2.0 by adding 10% sulfuric acid to prevent the loss of compounds for DOC analysis. Analyses of organic compounds in the bulk, permeate, and retentate of the solutions were performed using a DOC analyzer (DC-180, Dohrmann, USA). The concentrations of the ionic compounds were determined by conductivity measurements and were automatically corrected for temperature. The zeta potential of the RO, LPRO, NF membranes was measured at pH 3.5–9.5 and a NaCl concentration of 1000 mg/L using an electrokinetic analyzer apparatus (EKA, Brookhaven Instruments Corp., Holtsville, NY, USA) following an established procedure [23].

3. Results and discussion

3.1. RO and NF membrane characterization

In order to initially compare the basic properties of the RO (AK, ESPA, AG, 70LW, CAP, and LFC) and NF (HL and ESNA) membranes, solute rejection measurements based upon electrical conductivity and DOC were carried out for NaCl, $(\text{NH}_4)_2\text{CO}_3$, and urea solutions for a volumetric concentration factor of 2.5 at pH 7. To determine the most suitable membranes, the rejections of NaCl, $(\text{NH}_4)_2\text{CO}_3$, and urea are plotted as a function of permeate flux in Fig. 1. When choosing a membrane to produce drinking water, it is optimal to produce high-quality water with a high permeation rate, corresponding to the upper right hand corner of each graph in the figure. The HL (NF) membrane has the highest permeate flux, but it has the lowest rejection of solutes. The LFC (RO) membrane has the lowest flux, but this does not guarantee the highest rejection of solutes. Three membranes show promise based on the rejection of NaCl and $(\text{NH}_4)_2\text{CO}_3$ alone: AK, ESPA, and ESNA membranes. In addition, the AK membrane has good rejection and flux characteristics based on removal of urea, although the urea rejection is very low compared to the ions. This is because urea is a very small, uncharged molecule (MW 60.1 g/mol), so it is very difficult to reject by size exclusion and cannot be rejected by charge exclusion. Error bars based upon the standard deviation calculated from triplicate measurements of the rejection are quite small, so they are barely visible in the figure.

Producing both high permeate flux and high permeate quality has always been an issue in membrane filtration for potable water. Therefore, it is very important to evaluate

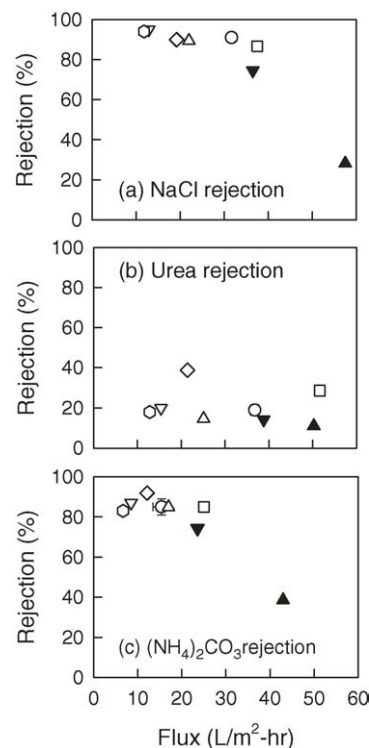


Fig. 1. Comparison of flux and solute rejection by RO and NF membranes. Operating conditions: $\Delta P = 800$ kPa; stirring speed = 400 rpm; $f_c = 2.5$. ((□) AK; (○) ESPA; (△) AG; (◇) 70LW; (▽) CAP; (⊙) LFC; (▲) HL; (▼) ESNA).

membrane permeate flux for various solutions. For the inorganic and organic compounds the permeate flux follows the order, urea > NaCl > $(\text{NH}_4)_2\text{CO}_3$, as shown in Fig. 1. Significant flux declines ranging from 9 to 73% of the pure water flux were observed, depending on the membrane and the water composition. The $(\text{NH}_4)_2\text{CO}_3$ solution showed a greater flux decline (45–73%) than the NaCl solution (19–46%) or the urea solution (9–36%). For the inorganic solutions this is because the $(\text{NH}_4)_2\text{CO}_3$ solution concentration (3429 mg/L) was greater than that for the NaCl solution (1000 mg/L) and had the higher osmotic pressure, which lowers flux by reducing the effective transmembrane pressure. However, the urea solution showed the lowest flux decline even though this contains the highest initial concentration, because the urea solution had the lowest final concentration in the concentrate compared with $(\text{NH}_4)_2\text{CO}_3$ and NaCl.

Fig. 2 shows the flux as a function of volumetric concentration factor for the filtration of solutions of urea and $(\text{NH}_4)_2\text{CO}_3$. Clearly, the permeate flux for the solutions was significantly reduced with increasing volumetric concentration factor. The $(\text{NH}_4)_2\text{CO}_3$ solution showed a greater flux decline than the urea solution. This is because not only was the initial $(\text{NH}_4)_2\text{CO}_3$ solution concentration (3429 mg/L) greater than that for the urea solution (2000 mg/L) at a volumetric concentration factor of 1.0, but also its final concentration was higher in the concentrate than that in the urea concentrate at a volumetric concentration factor of 2.5. In

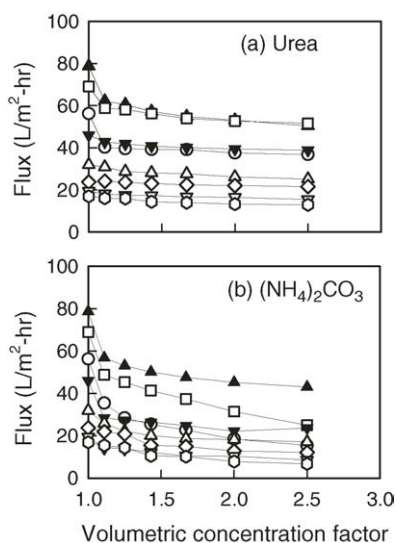


Fig. 2. Flux decline for reverse osmosis and nanofiltration of solutions containing (a) urea and (b) $(\text{NH}_4)_2\text{CO}_3$ for different membranes. Operating conditions: $\Delta P = 800$ kPa; stirring speed = 400 rpm; $f_c = 1.0$ –2.5. (\square) AK; (\circ) ESPA; (Δ) AG; (\diamond) 70LW; (∇) CAP; (\circ) LFC; (\blacktriangle) HL; (\blacktriangledown) ESNA.

addition, for $(\text{NH}_4)_2\text{CO}_3$ the AK and ESPA membranes had greater flux declines than the other membranes, since these RO membranes had higher ion rejections. This can be attributed to a higher osmotic pressure at the membrane surface, which reduces the effective transmembrane pressure.

3.2. Effect of pH on solute rejection

We focus on three membranes for the remainder of this study, one in each of the categories that we considered that provide the best rejection and flux based upon the screening study: AK (RO), ESPA (LPRO), and ESNA (NF). However, surface waters and wastewater effluents being treated for use as drinking water have complex compositions with various pH levels. Thus, it is important to consider the effect of solution pH on solute rejection. As shown in Fig. 3, the rejection of ionic solutes by the RO, LPRO, and NF membranes is dependent on the solution pH. For ionic salts (NaCl and $(\text{NH}_4)_2\text{CO}_3$) the RO and LPRO membranes with small pore sizes (the measurement of which will be discussed later) had a greater rejection than the NF membrane, indicating that size exclusion is at least partially responsible for the rejection. In addition, the rejection of these ionic solutes increases as the solution pH is increased from 3.5 to 7.5. A further increase in the pH, however, results in increased rejection for NaCl and slightly decreased rejection for $(\text{NH}_4)_2\text{CO}_3$. These results can be explained by electrostatic exclusion. The membrane charge becomes more negative with increasing pH, as shown in Fig. 4, resulting in increased electrostatic repulsion between Na^+/Cl^- ions and the membranes thus increasing the NaCl rejection. However, for $(\text{NH}_4)_2\text{CO}_3$ the equilibrium characteristics of ammonia (NH_3) with ammonium ions (NH_4^+) and bicarbonate (HCO_3^-) with carbonate

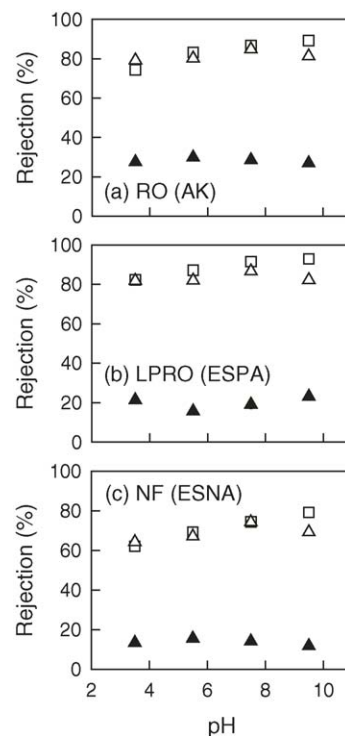


Fig. 3. Variation of solute rejection with respect to feed pH for RO (AK), LPRO (ESPA), and NF (ESNA) membranes. Operating conditions: $\Delta P = 800$ kPa; stirring speed = 400 rpm; $f_c = 2.5$. (\square) NaCl; (\blacktriangle) urea; (Δ) $(\text{NH}_4)_2\text{CO}_3$.

CO_3^{2-} ions play a role. At pH 9.5, the dominant form of nitrogen compounds is ammonia, which is an uncharged molecule and difficult to reject by the membranes. However, the dominant form of carbonate compounds is divalent CO_3^{2-} ions at the high pH, which is more easily rejected by the charged membranes compared to HCO_3^- ions, which are more dominant at lower pH. Apparently, the dominant effect is the reduced rejection due to the presence of ammonia. Therefore,

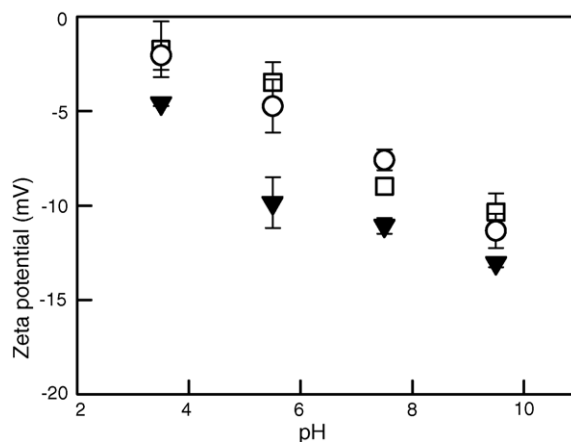


Fig. 4. Dependence of zeta potential on pH for RO (AK), LPRO (ESPA), and NF (ESNA) membranes. (NaCl = 1000 mg/L; (\square) RO; (\circ) LPRO; (\blacktriangledown) NF). Error bars are calculated based upon the standard deviation from triplicate measurements of the zeta potential.

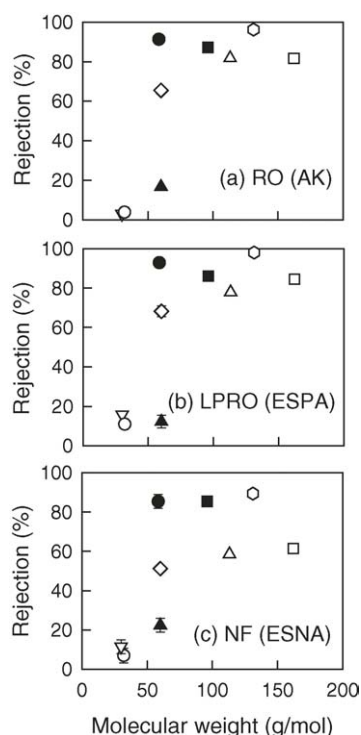


Fig. 5. Rejection of different compounds for RO and NF membranes. Operating conditions: $\Delta P = 800$ kPa; stirring speed = 400 rpm; feed concentration = 1 mM; $f_c = 2.5$. (a) RO (AK), (b) LPRO (ESPA), and (c) NF (ESNA). (■) ammonium carbonate; (●) sodium chloride; (▲) urea; (□) 2-(2-butoxyethoxy)ethanol; (△) caprolactam; (○) creatine; (∇) formaldehyde; (○) methanol; (◇) 2-propanol.

the overall rejection of $(\text{NH}_4)_2\text{CO}_3$ at pH 9.5 is slightly lower than that at pH 7.5. The rejection of urea by all the membranes was substantially lower than the ion rejection. The urea rejection varied somewhat in the pH range, as shown in Fig. 3, although it is unclear why this occurs. The rejection of urea, a small and uncharged molecule having no ionizable functional groups, should not be influenced by solution pH and membrane charge.

3.3. Comparison of solute rejections by selected RO, LPRO, and NF membranes

The rejection of both organic and inorganic compounds for the RO, LPRO, and NF membranes is shown in Fig. 5 as a function of the molecular weight of the rejected species. The rejection of the compounds was very similar between the RO (AK) and LPRO (ESPA) membranes except formaldehyde and methanol. The rejection was somewhat lower for the NF (ESNA) membrane than for the RO and LPRO membranes. Generally, higher molecular weight compounds have better rejection than low molecular weight compounds. However, the rejection is not purely a function of molecular weight. For instance, the rejection of creatine (MW 131.2 g/mol) was over 96% for the RO (AK) and LPRO (ESPA) membranes. However, the rejection of 2-(2-butoxyethoxy)ethanol (BEE), a molecule with a higher molecular weight (MW 162.2 g/mol),

was only approximately 80% for the RO and LPRO membranes. That the rejection of creatine is greater than that of BEE even though the molecular weight of creatine is smaller than that of BEE can be explained in terms of the solute radius of the molecules. The solute radii, which are listed in Table 2, can be calculated based upon the compounds' diffusion coefficient values (also shown in Table 2) using the Stokes–Einstein equation [24]:

$$D_i = \frac{k_B T}{6\pi\mu r_{i,s}} \quad (3)$$

where D_i is the diffusion coefficient of solute i , k_B is the Boltzmann constant, T is the temperature, μ is the solvent viscosity, and $r_{i,s}$ is the radius of solute i . Using this approach, the solute radius ($r_{i,s}$) of creatine is greater (0.37 nm) than that of BEE (0.32 nm) thus explaining the higher rejection of creatine. The rejection by the NF (ESNA) membrane is slightly lower for creatine (89%) and substantially lower for caprolactam (59%) and BEE (62%) compared to the RO and LPRO membranes, suggesting a larger effective pore size for the NF membrane.

For the relatively small organic compounds the rejection of 2-propanol is over 65% for the RO and LPRO membranes and nearly 50% for the NF membrane. Urea rejection (under 22%) is substantially lower than all the other compounds except formaldehyde and methanol (rejection under 15%). Urea, formaldehyde, and methanol are small or uncharged, so they are difficult to reject by size exclusion and by charge exclusion for all of the membranes. In addition, the rejection of urea is substantially lower than that of 2-propanol, even though they have identical molecular weights of 60.1 g/mol. This is because the solute radius of urea (0.18 nm) is smaller than that of 2-propanol (0.26 nm). These results suggest that the solute radius is a better parameter to predict the rejection of solutes than the molecular weight.

For ionic compounds the rejection of NaCl and $(\text{NH}_4)_2\text{CO}_3$ is high (over 85%) for all the membranes, even though the molecular weights of the ionic compounds (58.5 g/mol for NaCl and 96.1 g/mol for $(\text{NH}_4)_2\text{CO}_3$) are much smaller than creatine, caprolactam, and BEE. Clearly, the rejections of ions are governed mainly by electrostatic exclusion. In addition, the rejection of 2-propanol is substantially lower than that for NaCl, even though these compounds have similar molecular weight. This is because size exclusion is dominant for the 2-propanol rejection, while the rejection of NaCl is governed by both size exclusion and electrostatic exclusion.

3.4. Relationship between rejection and the ratio of solute radius to effective membrane pore radius

It is useful to consider the physical properties of both the solute and the membrane in order to understand rejection mechanisms for RO and NF membranes. For organic compounds, the hydrated radius, which is influenced by both solute shape and molecular weight, is the crucial parameter to

be considered. The size exclusion mechanism can be considered in terms of the dependence of the rejection on the ratio of the solute radius ($r_{i,s}$) to effective membrane pore radius (r_p). The rejection data for uncharged molecules (creatine, BEE, caprolactam, 2-propanol, formaldehyde, methanol, and urea) can be used to calculate the effective pore radius for each membrane based upon a model of steric interaction of hard spheres in cylindrical pores. Although this approach has been described in some detail elsewhere [8,13], we briefly summarize some key equations. It can be shown [13,26] that:

$$C_p = \frac{C_m K_{i,c} \phi}{1 - \exp\left(-\frac{K_{i,c} J_v \Delta x}{K_{i,d} D_i A_k}\right) (1 - \phi K_{i,c})} \quad (4)$$

$$c_i(x) = \left(\phi C_m - \frac{C_p}{K_{i,c}}\right) \exp\left(-\frac{K_{i,c} J_v x}{K_{i,d} D_i A_k}\right) + \frac{C_p}{K_{i,c}} \quad (5)$$

where C_m is the solute concentration at membrane surface on the concentrate side of the membrane, $K_{i,c}$ the hindrance factor for convection, ϕ the steric partition, $K_{i,d}$ the hindrance factor for diffusion, J_v the solvent flux through the membrane, Δx the membrane thickness, A_k the effective porosity of the membrane, c_i the solute concentration, and x the coordinate in the flow direction through the membrane. In these equations the effective membrane pore radius is hidden in the factors ϕ , $K_{i,c}$, and $K_{i,d}$, which are functions of the ratio of solute radius to effective membrane pore radius, $r_{i,s}/r_p$; ϕ and $K_{i,c}$ decrease with increasing $r_{i,s}/r_p$ ratio, while $K_{i,d}$ increases with increasing $r_{i,s}/r_p$ ratio. The solute concentration at the membrane surface, C_m , can be related to the experimental values of C_p , C_f , and J_v along with the estimated mass transfer coefficient, k , using the concentration polarization model based upon back diffusion of the solute from the membrane to the bulk solution [24],

$$\frac{C_m - C_p}{C_f - C_p} = e^{J_v/k} \quad (6)$$

The standard expression for the mass transfer coefficient in a stirred cell is [24],

$$k = 0.104 \left(\frac{D_{\text{eff}}}{r}\right) \left(\frac{\omega r^2 \rho}{\mu}\right)^{2/3} \left(\frac{\mu}{\rho D_{\text{eff}}}\right)^{1/3} \quad (7)$$

where D_{eff} is the effective diffusion coefficient, r the stirring radius, ω the stirring velocity, and ρ the solution density. Then using Eqs. (4) and (5), the two unknown parameters, r_p and $\Delta x/A_k$, can be calculated from the rejection data for each organic compound.

The calculated values of r_p based upon the rejection of each of the organic compounds are provided in Table 3. The estimated effective pore radii are consistent regardless of which organic compound they are based upon. The average effective pore radii r_p of the membranes were 0.33 nm for the RO, 0.34 nm for the LPRO, and 0.44 nm for the NF membranes. The values of r_p for the RO, LPRO, and NF membranes obtained in this analysis are similar to a previous

Table 3

Effective membrane pore size, r_p (nm), for the various organic compounds

	RO (AK)	LPRO (ESPA)	NF (ESNA)
Creatine	0.328	0.334	0.427
BEE	0.333	0.329	0.428
Caprolactam	0.327	0.328	0.427
2-Propanol	0.334	0.349	0.452
Formaldehyde	0.335	0.334	0.446
Methanol	0.344	0.336	0.452
Urea	0.329	0.343	0.448
Average	0.333	0.336	0.440

report using urea and creatine only (0.35, 0.35, and 0.45 nm, respectively) [13].

The availability of the membrane pore size allows a more meaningful analysis of the physical basis for the rejection using the ratio of solute radius to effective membrane pore radius, $r_{i,s}/r_p$, rather than simply the molecular weight of the species. The rejections of organic compounds are plotted as a function of $r_{i,s}/r_p$ for all three membranes in Fig. 6. In the figure, the data points having zero rejection correspond to water molecules (H_2O) with an assumption that water passed readily through the membrane pores. The data points for the RO and LPRO membranes can be identified for a particular compound, since they have almost identical $r_{i,s}/r_p$ ratios, whereas the ratio for the NF membrane is lower. The regression curve in the figure (solid curve) is based upon the measured rejection for all organic compounds for all the membranes such that:

$$R_i (\%) = (1 - e^{-K(r_{i,s}/r_p)^a}) \times 100 \quad (8)$$

where K (4.28) and a (1.97) are the fitting constants (valid for $r_{i,s}/r_p \geq 0.46$). The form of the regression curve was chosen so that the rejection asymptotically approaches 100% as $r_{i,s}/r_p$ increases. Clearly, a higher rejection occurs when the $r_{i,s}/r_p$ ratio increases. However, the prediction is imperfect in the region of the steepest part of the curve ($0.4 \leq r_{i,s}/r_p \leq 0.7$) in which the rejections of formaldehyde, methanol, and urea are quite low (<22%) for all the membranes. In addition, in

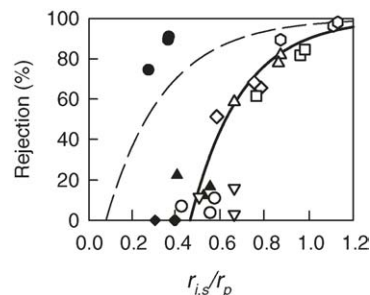
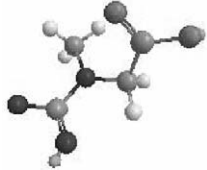
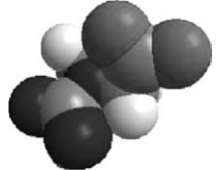
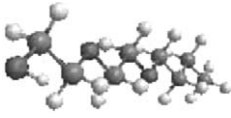
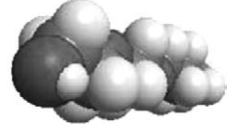

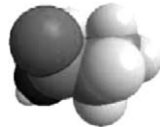
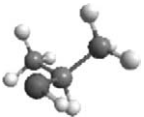





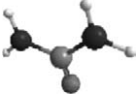





Fig. 6. Effect of solute radius/effective membrane pore radius on the rejection of various compounds by RO (AK), LPRO (ESPA), and NF (ESNA) membranes. Operating conditions: $\Delta P = 800$ kPa; stirring speed = 400 rpm; $f_c = 2.5$. ((●) sodium chloride; (▲) urea; (□) 2-(2-butoxyethoxy)ethanol; (△) caprolactam; (○) creatine; (▽) formaldehyde; (○) methanol; (◇) 2-propanol; (◆) water). Solid curve: regression fit to data for organic compounds (Eq. (8)); dashed curve: regression fit for inorganic compounds [28].

Table 4
Three dimensional molecular structures of the organic compounds and water [based upon Chem3D]

Compound	Ball-and-stick	Space-filling
Creatine		
2-(2-Butoxyethoxy) ethanol		
Caprolactam		
2-Propanol		
Formaldehyde		
Methanol		
Urea		
Water		

By manually adjusting the scale so that the oxygen atoms are similar in size for all molecules, the molecules appear at approximately the same scale to allow comparison of the overall size of the molecules.

the same region the rejection of formaldehyde and methanol by the RO and LPRO membranes was much lower (<16%) than that of caprolactam and 2-propanol by the NF membrane (>51%), even though formaldehyde and methanol for the RO and LPRO membranes and caprolactam and 2-propanol for the NF membrane have similar $r_{i,s}/r_p$ ratios (ranging from 0.55 to 0.66). This may be a consequence of different degrees of steric exclusion, since these compounds have different molecular structures. The three dimensional molecular structures of all the organic compounds that were considered are shown in Table 4 (obtained using commercially available software: Chem3D, CambridgeSoft Corp., Cambridge, MA, USA). The space-filling models show the size and position of the atoms based upon the bonding properties and van der Waals radius [27]. Although the space-filling models are most realistic, the ball-and-stick models depict the molecular structure more clearly. Formaldehyde and methanol have smaller and less complex three-dimensional structures than

caprolactam and 2-propanol. This may lead to better transport of formaldehyde and methanol through the RO and LPRO membranes than caprolactam and 2-propanol through the NF membrane in spite of similar $r_{i,s}/r_p$ ratios. Apparently, the more complex molecules, caprolactam and 2-propanol, are rejected more easily by steric exclusion than formaldehyde and methanol. Thus, the structure of compounds may need to be considered for the rejection of organic compounds in addition to the $r_{i,s}/r_p$ ratio. When the $r_{i,s}/r_p$ ratio is greater than 0.7, the collapse of the data is much better than at lower ratios. The compounds at the higher ratios, creatine, BEE, and caprolactam, all have large solute radii. However, their structures differ substantially. Creatine is a compact chain, BEE is a long chain, and caprolactam is a ring. Thus, it appears that the rejection depends primarily upon the molecular size, and the molecular structure is less important for these larger molecules. From the results one could categorize the rejection of organic compounds into three classes according

to the ratio, $r_{i,s}/r_p$. At the lowest ratios, $r_{i,s}/r_p < 0.4$, the rejection is negligible. At moderate ratios, $0.4 \leq r_{i,s}/r_p \leq 0.7$, the rejection can be either quite low or moderate, depending upon the structure of the solute and the resulting steric exclusion. At high ratios, $r_{i,s}/r_p > 0.7$, the rejection seems dependent only on the $r_{i,s}/r_p$ ratio with little effect due to the solute's molecular structure.

The rejection of an ionic solute (NaCl) is also shown in Fig. 6 (filled circle symbols). The NaCl rejection is much greater than that for the organic compounds even at lower $r_{i,s}/r_p$ ratios. In addition, the dependence of the rejection on $r_{i,s}/r_p$ for various ionic solutes (at very high concentrations) including potassium, calcium, magnesium, phosphate, sulfate, ammonium, nitrate, and nitrate ions as well as sodium and chloride ions obtained from our study for the same RO, LPRO, and NF membranes [28] is shown in Fig. 6 for comparison (dashed curve). The rejection of the ionic solutes is much greater than that for the organic compounds at the same $r_{i,s}/r_p$ ratios, verifying that the rejection of a charged compound is governed by electrostatic exclusion in addition to steric exclusion. (The data points in Fig. 6 for NaCl are somewhat above the dashed curve, because the concentration used here is substantially lower than that in the other work.)

3.5. Rejection mechanisms: diffusion, electromigration, and convection

Since solute transport through RO and NF membrane pores is influenced by solute concentration at the membrane surface, determining solute concentration at the membrane surface is important to understanding solute rejection by RO and NF membranes. Fig. 7 shows the ratios of solute concentration on membrane surface (C_m), calculated using Eq. (5), to bulk concentration (C_f) for all of the solutes for the three membranes. The RO membrane has a higher C_m/C_f ratio because of its higher flux and high rejection. The NF membrane exhibits a lower C_m/C_f ratio than the RO and LPRO membranes. This is because for all the solutions of 1 mM (30–162 mg/L) the membrane permeability of the NF membrane is lower (Table 1) and the rejection of most of

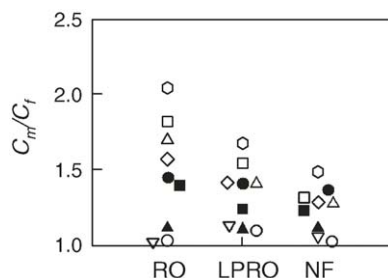


Fig. 7. Ratio of the solute concentration on the membrane surface to bulk concentration for RO (AK), LPRO (ESPA), and NF (ESNA) membranes. Operating conditions: $\Delta P = 800$ kPa; stirring speed = 400 rpm; feed concentration = 1 mM; $f_c = 2.5$. (■) ammonium carbonate; (●) sodium chloride; (▲) urea; (□) 2-(2-butoxyethoxy)ethanol; (△) caprolactam; (○) creatine; (▽) formaldehyde; (◇) methanol; (◇) 2-propanol.

the compounds is lower than the RO and LPRO membranes. The C_m/C_f ratio for all the membranes is higher for creatine, BEE, caprolactam, and 2-propanol than that for urea, formaldehyde, and methanol due to the higher rejection of the larger molecules. However, the C_m/C_f ratio for NaCl and $(\text{NH}_4)_2\text{CO}_3$ is lower than that for creatine and BEE for the RO and LPRO membranes, even though they have the similar rejections. This is because the effective diffusion coefficient of NaCl and $(\text{NH}_4)_2\text{CO}_3$ is higher than that of creatine and BEE.

The relative importance of various transport mechanisms for solute through the membranes can be determined using a transport model based upon the extended Nernst–Planck Equation combined with a concentration polarization model [13,26,29]:

$$J_i = -K_{i,d}D_i \frac{dc_i}{dx} - c_i \frac{z_i K_{i,d} D_i F}{RT} \frac{d\psi_m}{dx} + K_{i,c} J_v c_i \quad (9)$$

where J_i is the solute flux, z_i the valency of solute i , F the Faraday constant, ψ_m the membrane potential, and R the gas constant. The terms on the right hand side represent transport due to diffusion, the electric field gradient, and convection, respectively. Based upon the Nernst–Planck equation, Bowen and Mohammad [26] suggested that the contribution of each transport mechanism in the membrane can be approximated using a one-step central difference estimate of the gradient. For uncharged organic compounds, the contribution by electromigration is zero because the valency of compound, z_i , is zero in Eq. (9). Thus, solute transport depends only upon the diffusion and convection. The following expressions reflect the percentage contribution of each transport mechanism in Eq. (9) to the total transport:

$$\text{Diffusion (\%)} = \frac{1}{J_i} \left(-K_{i,d} D_i \frac{C_p - C_m}{\Delta x} \right) \times 100 \quad (10)$$

$$\text{Convection (\%)} = \frac{1}{J_i} \left(K_{i,c} J_v \frac{C_m + C_p}{2} \right) \times 100 \quad (11)$$

The diffusion coefficient and the ratio of solute radius to effective membrane pore radius, $r_{i,s}/r_p$, play a role in the hindrance factor for both transport mechanisms. In the above equations for diffusion and convection, $K_{i,d}$, $K_{i,c}$, and D_i are known parameters for each solute or membrane, J_i , J_v , and C_p are based upon experimental data obtained from the stirred cell tests, and C_m is calculated from Eq. (6). The contributions of diffusion and convection are shown in Fig. 8 as a function of the diffusion coefficient and the $r_{i,s}/r_p$ ratio. The mass transport through the membrane is controlled mainly by diffusion for membrane/compound combinations that have a high $r_{i,s}/r_p$ ratio (>0.75). In these cases, the convective transport is minimal and the rejection of solute is high. Since the solute concentration on the high-pressure side of the membrane is much greater than that on the low-pressure side, diffusion dominates. However, the contribution of convection is dominant for membrane/compound combinations that have a small $r_{i,s}/r_p$ ratio, since J_v and $K_{i,c}$ increase with decrease-

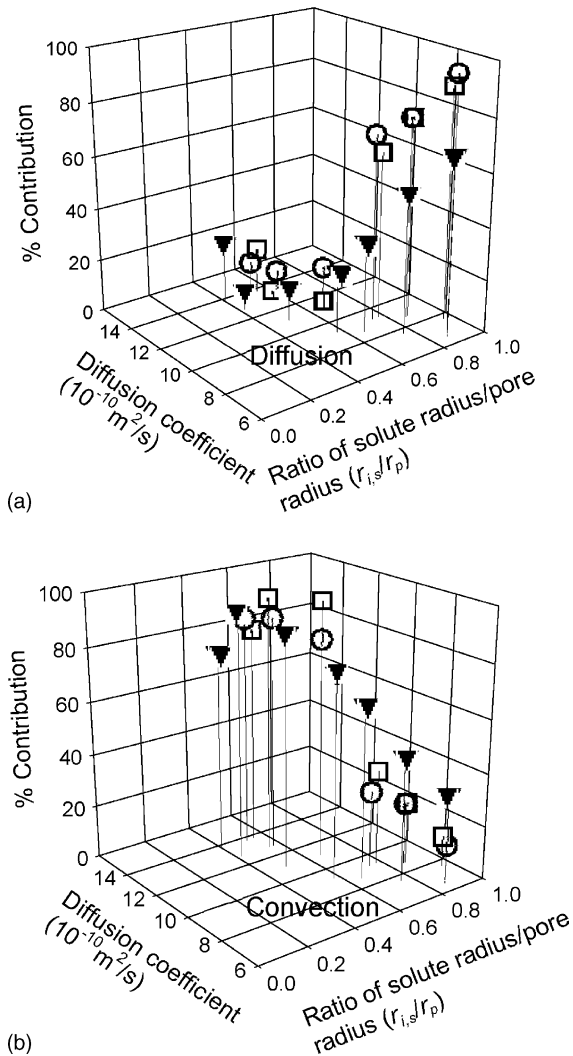


Fig. 8. Relative contribution of transport mechanisms for RO (AK), LPRO (ESPA), and NF (ESNA) membranes with different organic compounds (urea, 2-(2-butoxyethoxy)ethanol, caprolactam, creatine, formaldehyde, methanol, and 2-propanol). (a) Diffusion and (b) convection. (□) RO; (○) LPRO; (▼) NF.

ing $r_{i,s}/r_p$ ratio. The contributions obtained in this analysis for creatine are similar to those in a previous report for the LPRO (ESPA) membrane [13].

4. Conclusions

Commercially available RO and NF membranes were tested to determine rejection of organic and inorganic compounds using laboratory scale experiments. The results show that rejection of organic compounds and ions by RO membranes was higher than NF membranes due to size exclusion, since the RO membranes have smaller membrane pore radii than the NF membrane. To better understand the rejection mechanisms (size exclusion and electrostatic exclusion), the ratio of solute radius ($r_{i,s}$) to effective membrane pore radius (r_p) was employed to compare the rejections. For all the or-

ganic compounds, the rejection depends upon the $r_{i,s}/r_p$ ratio for the RO, LPRO, and NF membranes. Significant rejection occurs when the $r_{i,s}/r_p$ ratio is greater than 0.8. However, for the three membranes the prediction of rejection given by Eq. (8) and shown in Fig. 6 is imperfect for $r_{i,s}/r_p$ ratios between 0.4 and 0.7. Apparently, the rejection of organic compounds in this range of $r_{i,s}/r_p$ ratios depends upon the molecular structure in addition to the $r_{i,s}/r_p$ ratio. The rejection of NaCl is much higher than that for the organic compounds at the same $r_{i,s}/r_p$ ratio, indicating that the rejection of ionic compounds is governed by electrostatic repulsion. For organic compounds the transport of solutes is controlled by diffusion and convection. The contribution by diffusion is dominant for the compounds having a high $r_{i,s}/r_p$ ratio, while the contribution of convection is dominant for compounds having a small $r_{i,s}/r_p$ ratio.

Acknowledgements

This work was supported by National Aeronautics and Space Administration (NASA). The authors thank Hydraulics Inc. and Toray Industries Inc. for their donation of membrane samples. The authors also thank Richard Neal for his help in performing a number of rejection measurements.

Nomenclature

a	fitting constant (–)
A_k	effective porosity of membrane (–)
c_i	solute concentration inside membrane phase (mol/m ³)
C_f	solute concentration in feed (bulk) solution (mol/m ³)
C_m	solute concentration at membrane surface (mol/m ³)
C_p	solute concentration in permeate solution (mol/m ³)
D_i	diffusion coefficient of solute i (m ² /s)
D_{eff}	effective diffusion coefficient of solute (m ² /s)
f_c	volumetric concentration factor (–)
F	Faraday constant (C/mol)
J_i	solute flux through membrane (m/s)
J_v	solvent flux through membrane (m/s)
k	mass transfer coefficient on high-pressure side of membrane (m/s)
k_B	Boltzmann constant (J/K)
K	fitting constant (–)
$K_{i,c}$	hindrance factor for convection (–)
$K_{i,d}$	hindrance factor for diffusion (–)
r	radius of stirred cell (m)
r_p	effective pore radius of membrane (m)
$r_{i,s}$	radius of solute i (m)

R	gas constant (J/mol K)
R_i	rejection for solute i (–)
T	temperature (K)
V_c	volume of concentrate (m^3)
V_f	volume of initial feed (m^3)
V_p	volume of permeate (m^3)
x	coordinate in flow direction (m)
Δx	membrane thickness (m)
z_i	valency of solute i (–)

Greek symbols

μ	solvent viscosity (kg/m s)
π	mathematical constant (–)
ρ	solution density (kg/m^3)
ϕ	steric partitioning term (–)
Ψ_m	electrical potential in membrane phase (V)
ω	stirring velocity (rad/s)

References

- [1] S.A. Snyder, P. Westerhoff, Y. Yoon, D.L. Sedlak, Pharmaceuticals, personal care products, and endocrine disruptors in water: implications for the water industry, *Environ. Eng. Sci.* 20 (2003) 449–469.
- [2] J.E. Drewes, M. Reinhard, P. Fox, Comparing microfiltration-reverse osmosis and soil-aquifer treatment for indirect potable reuse of water, *Water Res.* 37 (2003) 3612–3621.
- [3] W.H. Peng, I.C. Escobar, D.B. White, Effects of water chemistries and properties of membrane on the performance and fouling—a model development study, *J. Membr. Sci.* 238 (2004) 33–46.
- [4] N.M. Al-Bastaki, Performance of advanced methods for treatment of wastewater: UV/TiO₂, RO and UF, *Chem. Eng. Process* 43 (2004) 935–940.
- [5] Y. Kiso, Y. Nishimura, T. Kitao, K. Nishimura, Rejection properties of non-phenylic pesticides with nanofiltration membranes, *J. Membr. Sci.* 171 (2000) 229–237.
- [6] Y. Kiso, Y. Sugiura, T. Kitao, K. Nishimura, Effects of hydrophobicity and molecular size on rejection of aromatic pesticides with nanofiltration membranes, *J. Membr. Sci.* 192 (2001) 1–10.
- [7] L.D. Nghiem, A.I. Schafer, T.D. Waite, Adsorptive interactions between membranes and trace contaminants, *Desalination* 147 (2002) 269–274.
- [8] L.D. Nghiem, A.I. Schafer, M. Elimelech, Removal of natural hormones by nanofiltration membranes: measurement, modeling, and mechanisms, *Environ. Sci. Technol.* 38 (2004) 1888–1896.
- [9] L.D. Nghiem, A. Manis, K. Soldenhoff, A.I. Schafer, Estrogenic hormone removal from wastewater using NF/RO membranes, *J. Membr. Sci.* 242 (2004) 37–45.
- [10] A.I. Schafer, L.D. Nghiem, T.D. Waite, Removal of the natural hormone estrone from aqueous solutions using nanofiltration and reverse osmosis, *Environ. Sci. Technol.* 37 (2003) 182–188.
- [11] S. Lee, R.M. Lueptow, Toward a reverse osmosis membrane system for recycling space mission wastewater, *Life Support Biosph. Sci.* 7 (2000) 251–261.
- [12] S. Lee, R.M. Lueptow, Reverse osmosis filtration for space mission wastewater: membrane properties and operating conditions, *J. Membr. Sci.* 182 (2001) 77–90.
- [13] S. Lee, R.M. Lueptow, Membrane rejection of nitrogen compounds, *Environ. Sci. Technol.* 35 (2001) 3008–3018.
- [14] A.E. Childress, M. Elimelech, Effect of solution chemistry on the surface charge of polymeric reverse osmosis and nanofiltration membranes, *J. Membr. Sci.* 119 (1996) 253–268.
- [15] Y. Yoon, G. Amy, J. Cho, J. Pellegrino, Systematic bench-scale assessment of perchlorate rejection mechanisms by nanofiltration and ultrafiltration membranes, *Sep. Sci. Technol.* 39 (2004) 2105–2135.
- [16] L. Lin, K.C. Rhee, S.S. Koseoglu, Bench-scale membrane degumming of crude vegetable oil: process optimization, *J. Membr. Sci.* 134 (1997) 101–108.
- [17] B.W. Finger, L.N. Supra, L. DallBauman, K.D. Pickering, Development and testing of membrane biological wastewater processors, International Conference on Environmental Systems, SAE Paper 1999-01-1947, 1999.
- [18] J.L. Golden, Space station requirements for materials and processes, NASA report SSP 30233 Revision E, 1995.
- [19] C.E. Verostko, C. Carrier, B.W. Finger, Ersatz wastewater formulations for testing water recovery systems, SAE paper 2004-01-2448, 2004.
- [20] D. Rajkumar, K. Palanivelu, Electrochemical treatment of industrial wastewater, *J. Hazard. Mater.* 113 (2004) 125–131.
- [21] P. Fox, S. Ketha, Anaerobic treatment of high-sulfate wastewater and substrate interactions with isopropanol, *J. Environ. Eng. -ASCE* 122 (1996) 989–994.
- [22] K.J. Chae, S.K. Yim, K.H. Choi, Application of a sponge media (BioCube) process for upgrading and expansion of existing caprolactam wastewater treatment plant for nitrogen removal, *Water Sci. Technol.* 50 (2004) 163–171.
- [23] M.C. Wilbert, S. Delagah, J. Pellegrino, Variance of streaming potential measurements, *J. Membr. Sci.* 161 (1999) 247–261.
- [24] M. Mulder, Basic Principles of Membrane Technology, 2nd ed., Kluwer Academic Publishers, Dordrecht, The Netherlands, 1996.
- [25] D.R. Lide, CRC Handbook of Chemistry and Physics, 76th ed., CRC Press, Boca Raton, FL, USA, 1995.
- [26] W.R. Bowen, A.W. Mohammad, Characterization and prediction of nanofiltration membrane performance—a general assessment, *Chem. Eng. Res. Des.* 76 (1998) 885–893.
- [27] J.M. Berg, J.L. Tymoczko, L. Stryer, Biochemistry, 5th ed., W.H. Freeman, New York, NY, USA, 2002.
- [28] Y. Yoon, R.M. Lueptow, Reverse osmosis membrane rejection for ersatz space mission wastewaters, *Water Res.*, in review.
- [29] J. Schaep, C. Vandecasteele, A.W. Mohammad, W.R. Bowen, Analysis of the salt retention of nanofiltration membranes using the Donnan-steric partitioning pore model, *Sep. Sci. Technol.* 34 (1999) 3009–3030.